Springer

Journal of Mechanical Science and Technology 22 (2008) 1876~1882

Journal of Mechanical Science and Technology

www.springerlink.com/content/1738-494x
DOI 10.1007/s12206-008-0726-9

Performance of a cross-flow fan with various shapes of a rearguider and an exit duct †

Tae-An Kim[1], D.-W. Kim[2], S.-K. Park[2], and Youn J. Kim[1,*]

[1]*School of Mechanical Engineering, Sungkyunkwan University, 300 Cheoncheon-dong, Suwon 440-746, Korea*
[2]*Digital Appliance R & D Center, Samsung Electronics Co., Ltd., 416 Meatan3-dong, Suwon 442-742, Korea*

(Manuscript Received April 16, 2008; Revised July 7, 2008; Accepted July 23, 2008)

Abstract

A cross-flow fan having forward curved blades relatively produces higher dynamic pressure at low rotating speed because a working fluid passes through an impeller blade twice. Most of this dynamic pressure is transferred to the static pressure in a rearguider and a stabilizer as a scroll in the centrifugal fan. The effect of a rearguider and a stabilizer on the performance of a cross-flow fan is higher than that of the impeller. Therefore, it should be considered how the shape of a rearguider and an exit duct affects on the performance and the flow fields. The purpose of this study is to investigate the reciprocal relation to the flow field and performance among the design parameters. Two-dimensional, unsteady governing equations are solved using FVM algorithm, sliding grid system and standard $k-\varepsilon$ turbulence model. Velocity profiles with various parameters are depicted. Furthermore, the meridional velocity profiles around the impeller are plotted at fixed rotating speed and design flow rate.

Keywords: Archimedes spiral; Cross-flow fan; Rearguider; Stabilizer; Fan performance

1. Introduction

A cross-flow fan (hereafter CFF) consists of an impeller, a stabilizer and a rearguider. When it is applied to air conditioning systems, an evaporator should be added. CFF with those elements has been used in the wide range of industries: ventilating devices in mining, building, automobile, etc. It is recently adopted in the indoor units of an air conditioner as a home appliance. They are gradually slimmed because of a fine view and the pressure drop in CFF is larger than before. Then CFF is operated in the lower flow region and its operating stability is a very important subject.

A working fluid in CFF passes through the impeller blade twice and the impeller has a large absolute flow velocity because of a forward curved blade. This may reduce the rotating speed to achieve the equal pressure difference at the same flow rate, comparing with the other types such as radial and backward curved ones, and CFF can be applied to the small-size air conditioning systems. However, it is known that the efficiency of a blower is commonly higher when the backward curved blade angle (β_2) is larger. Typically, the efficiency of CFF having forward curved blades is 30 to 40% due to a large impact loss in blades.

There are two different vortices in the flow fields of CFF. One is an eccentric vortex, a forced vortex, induced by recirculation from the stabilizer to the impeller, and the other is the free vortex in the rearguider. Especially, the fan performance is directly influenced by the location of the eccentric vortex. There are several studies on shape parameters of components of CFF, but design theories like a turbo pump have not been established yet. Most of the studies have been carried out based on the reiterated case studies by empirical and numerical methods.

† This paper was presented at the 9th Asian International Conference on Fluid Machinery (AICFM9), Jeju, Korea, October 16-19, 2007.

*Corresponding author. Tel.: +82 31 290 7448, Fax.: +82 31 290 5889
E-mail address: yjkim@skku.edu

Eck [1] studied the flow characteristics of CFF using experimental and analytical methods. Especially, he investigated the forced and free vortices in CFF and visualized the occurrence of eccentric vortex in the impeller. He also studied the flow and noise characteristics with varying the shape of the stabilizer. Tsurusaki *et al*. [2] measured the internal flow velocity in CFF using PTV (particle tracking velocimetry). The path line and the velocity distribution were taken using a digital camera, and the generation and the diffusion of the vorticity induced by the eccentric vortex were calculated. Yamafuji and Nishihara [3] clarified the generation procedures of irregular main flow by LDV and disclosed the production of vortex shedding at a blade tip. It is verified that the principle of the eccentric vortex could be comprehended from those phenomena. Murada and Nishihara [4] inquired that the setting angle, the gaps between components and the rear guider shape are important design parameters of which affect to the fan performance. In case of a slight variation of Reynolds number with a little change on the diameter and the rotational velocity, it is published that the flow and pressure coefficients are valid by means of the study on the scale effect versus Reynolds number.

In general, the dynamic pressure is converted into the static pressure in a stabilizer and a rearguider as a scroll in the centrifugal fan. The impeller having forward curved blades generates higher dynamic pressure. Therefore, the flow behaviors in the stabilizer and the rearguider are more important than the other components.

In this study, the flow behavior and the performance of CFF are investigated for different rearguider shapes and stabilizer positions. Specifically, the reciprocal relations of the static pressure difference and the efficiency are studied.

2. Theoritical background

2.1 Design parameters

Design parameters and general specifications of the modeled CFF are shown in Fig. 1 and Table 1. In order to investigate the characteristics of the performance, dimensionless parameters, i.e., the pressure coefficient (ψ), the flow coefficient (ϕ) and the power coefficient (λ_p) are defined as follows:

$$\psi = \Delta p_s / \frac{1}{2}\rho U_2^2, \quad \phi = q / b_2 D_2 U_2, \quad \lambda_p = \psi\phi/\eta \qquad (1)$$

2.2 The curved part of a rearguider

The flow behavior of CFF has the same nature as that of a turbo pump because of the incompressibility of flows in the fan (M<0.3). Therefore, it is very important to design an optimal shape of the rearguider.

A working fluid acquires the energy, passing through impeller blades twice. Some particular part (θ_d) of the impeller only discharges air into the curved part of the rearguider. The shapes of the curved part (θ_4) are designed with a circular arc and two Archimedes spirals. Especially, that spiral shape is known to have excellent pressure recovery in the general scroll of turbomachinery. As mentioned before, flowing out within the restricted region of the impeller, the value of a discharge angle (θ_d) is not 360^o but empirical values. The relevant formula for the spiral is as follows:

$$r_4(\theta) = r_3 \exp[q_b\theta/(C_{\theta 2}\cdot r_2 \cdot b_2 \cdot \theta_d)] \qquad (2)$$

where,

$$r_3 = r_2 + \varepsilon_r,$$
$$C_{\theta 2} = \sigma(C_{m2}/\tan\beta_2),$$
$$\sigma = 1/\left(1+\sin(\pi-\beta_2)\frac{\pi}{Z_b(1-r_1/r_2)^2}\right).$$

Using the above formulas, Archimedes spirals were generated at design point (5 CMM). Two Archimedes spirals are distinguished from the starting angle (θ_{rs}) of the rearguider. As shown in Fig. 1, the difference of the starting angle ($\Delta\theta_{rs}$) between the first Archimedes spiral (hereafter 1st Ar) and the second Archimedes spiral (hereafter 2nd Ar) is 13.7^o. Each straight part of the rearguiders is a tangential line of the curved part.

Table 1. General parameters and operating conditions.

Impeller diameter, D_2	95 mm
Diameter ratio, D_1/D_2	0.76
Blade angles	β_1=90°, β_2=24.5°
Number of blade	35
Blade profile	Circular arc
Rotating speed	16.67 sec^{-1}
Re_C *(for blade chord length)*	4,490
Re_D *(for impeller diameter)*	31,458

2.3 Positions of the stabilizer

The stabilizer and the straight part of the rearguider constitute the exit duct performing as a channel diffuser (see Fig. 1). Then, changing the setting angle of the stabilizer (θ_{es}), the area ratio (AR) and the enlargement angle ($2\theta_e$) of the exit duct are varied as shown in Table 2. Especially, the setting angle is varied from 19° to 27° per 2° and the gap between the impeller and the stabilizer is fixed at 3.5 mm.

3. Numerical analysis

3.1 Governing equations

The conservative equations for two-dimensional, unsteady, turbulence and viscous flows are as follows:

$$\frac{1}{\sqrt{g}}\frac{\partial}{\partial t}(\sqrt{g}\rho)+\frac{\partial}{\partial x_j}(\rho u_j)=0 \tag{3}$$

$$\frac{1}{\sqrt{g}}\frac{\partial}{\partial t}(\sqrt{g}\rho u_i)+\frac{\partial}{\partial x_j}(\rho\tilde{u}_j u_i-\tau_{ij})=-\frac{\partial p}{\partial x_i}+S_i \tag{4}$$

where t is the time, $\sqrt{g}$ the matrix equation of a tensor, ρ the density, u the velocity and S_i the source of momentum, respectively.

These governing equations were discretized by the finite volume method (FVM) to find the solutions for flow variables. The hybrid scheme was used to handle the convection and diffusion terms in the governing equations. The standard $k-\varepsilon$ turbulence model with the wall function was adopted to simulate the behaviors of turbulence. Analyses were carried out until solutions reach a steady state.

3.2 Grid systems and boundary conditions

The multi-block method was used to form complicated geometries of CFF. The numerical domain consists of the inlet region, the impeller,, the rear guider and the exit duct (see Fig. 2). These are needed to solve the enhanced near each gap: ε_r (between the rearguider and the impeller) and commercial code, STAR-CD. Sliding grids provide with an interface between the rotating and stationary parts was event module made simulations of the unsteady and the rotating flow behaviors in interface. It does not change the original geometry and grid number, but varies the relative location of the grid to the stationary part. The grid system was made by the assumption

Table 2. Stabilizer positions.

θ_{es}	Radial (56 mm)		1st. Archimedes		2nd Archimedes	
	AR	$2\theta_e$	AR	$2\theta_e$	AR	$2\theta_e$
27°	1.22	6.2°	1.16	4.8°	1.18	5.5°
25°	1.33	8.4°	1.26	7.0°	1.46	12.9°
23°	1.46	10.4°	1.37	9.13°	1.59	14.9°
21°	1.62	12.5°	1.51	11.1°	1.76	17.1°
19°	1.82	14.3°	1.68	12.9°	1.95	19.0°

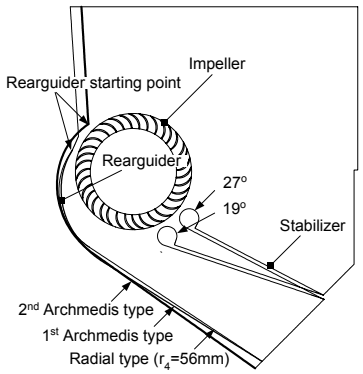

(a) Model of a cross-flow fan

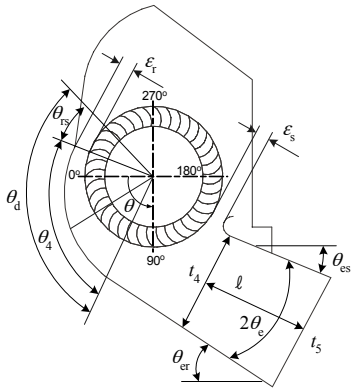

(b) Design parameters

Fig. 1. Schematic diagram and design parameters of a cross-flow fan.

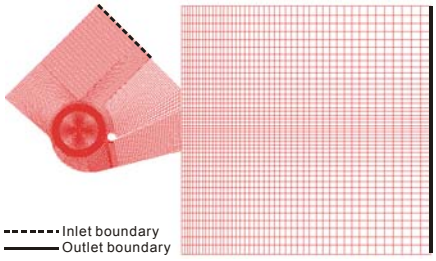

Fig. 2. Grid systems of the modeled cross-flow fan.

that the flow in CFF is two-dimensional. In order to minimize the error induced by the cell numbers, the grid number was increased to 80,000. However, there was no change in the value of flow variables in comparison with 65,000 cells. The number of cells was fixed at 65,000 to reduce the calculating time.

Pressure and outlet boundary conditions are respectively adopted for the inlet and the outlet boundaries as shown in Fig. 2. In this case, the pressure of the inlet boundary is set to the atmospheric pressure and the fixed flow rates are presented on the outlet boundary. The attachment boundary condition is used on the interface among the rotating cells near the impeller and the stationary cells. The rotating cells will be linked with the next fixed cells along the rotating direction and new regions will be produced at that time. In addition, no-slip condition is used on the wall boundary. It is presumed that there is no mass flux on walls. Wall functions are also employed to reduce the number of cells for calculating turbulence variables.

4. Experimental method

The experimental apparatus, the fan tester, was arranged to comply with ASHRAE standard 51-75. It is a front suction type as shown in Fig. 3. The static pressure produced by CFF is measured from static pressure taps at the upstream stabilization chamber of the fan tester. The micromanometer (SAMDUK, FCO510, error rate: ±0.25%) was used to record the pressure difference for measuring the flow rate. The volume flow rate is calculated from an empirical equation using the static pressure difference at the upstream and downstream of five nozzles located at the middle of the tester. Five nozzles were installed on the same plate as shown in Fig. 3. These are respectively opened or closed to set the operating flow rate. The uncertainty for the volume flow rate is ±2.83%. The power of the working motor connected to CFF is generally obtained by multiplying the torque of the fan shaft and the angular velocity after measuring those respectively using a torque meter and an rpm gauge. However, in this study, it was measured using the digital power meter (Yokogawa, WT1000 series) and corrected using the performance curve of the motor.

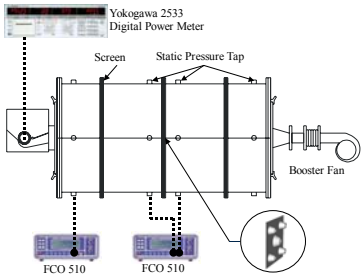

Fig. 3. Schematic diagram of a fan tester.

5. Results and discussion

In this study, the effects of the curved part of a rearguider and the position of a stabilizer on the performance and the flow fields of CFF are studied. First of all, in order to verify the numerical results, these are compared with the experiments. Comparisons were depicted in Fig. 4. The greatest difference of pressure occurred in the case of the 1st Ar and the next is the 2nd Ar and the last one is Radial type in both numerical and experimental results. Numerical results of the pressure difference between the Radial and 2nd Ar types are fairly similar to the experimental results. In the case of the 1st Ar, however, there exists a relatively large discrepancy between the results. This phenomenon may be caused by the 3D losses, such as the friction loss of the disc, and volumetric losses in the lateral gaps.

5.1 Numerical results

In order to elucidate the flow field in CFF in detail, the meridional velocity (C_{m2}) around the exit of impeller is presented in Fig. 5. Results are plotted by each rearguider at θ_{es}=21°. The positive value of velocity denotes that the fluid is discharged from the impeller. On the contrary, for a negative value, it de-

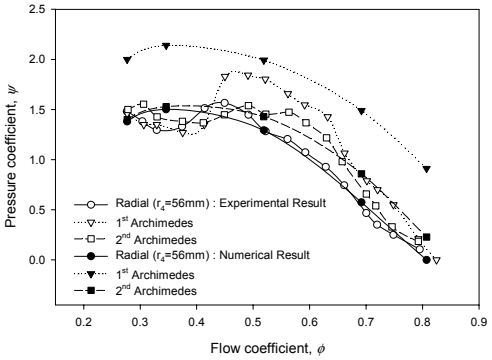

Fig. 4. Comparison of the pressure coefficients between the numerical (solid symbols) and experimental results (open symbols).

notes that the fluid is sucked. In the aspect of θ, the positions of stabilizer are located at 124.0° (θ_{es}=25°), 129.5° (θ_{es}=23°) and 135.0° (θ_{es}=21°) respectively. Besides, the starting angle of the rearguider is separately327.6° (for Radial and 1st Ar) and 313.9° (for 2nd Ar). The eccentric vortex occurred at 80°. Periphery flows around the impeller consist of suction, discharge, recirculation and diffusion. First, suction is formed on the right side of the impeller (θ = 120°-240°) and fluid is discharged to the left side (θ =0°-80° and 330°-360°). Diffusion occurred on the top (θ= 240°-330°) and recirculation region resulted form the eccentric vortex is on the bottom (θ= 80°-120°).

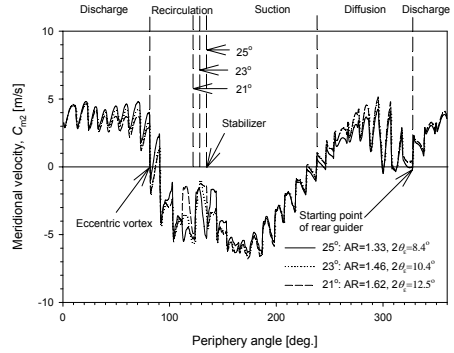

(a) Radial type rearguider

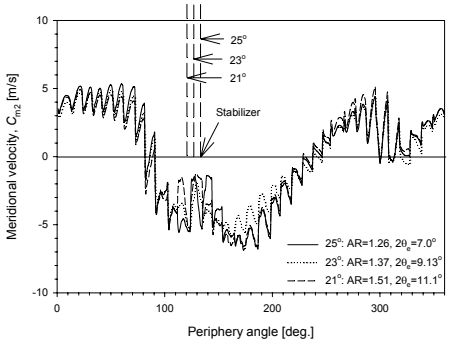

(b) 1st Archimedes type rearguider

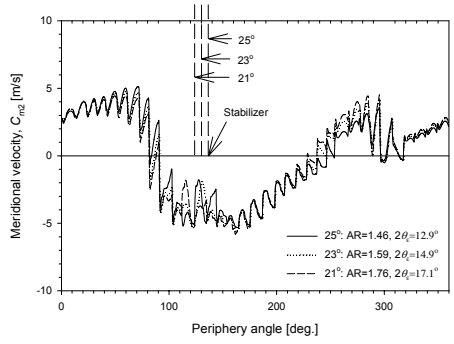

(c) 2nd Archimedes type rearguider

Fig. 5. Meridional velocity profiles around the impeller with different stabilizer positions.

The meridional velocity in the discharge region increases as θ increases in case of Archimedes spiral, but that is nearly fixed to a regular value. The phenomenon for 1st and 2nd Ar results from the characteristics of the Archimedes spiral. Archimedes spiral is designed to keep the vertical velocity identical for a cross-sectional area at θ (x). Therefore, the flow rate ($q_{\theta(x)} \propto C_{m2}$) and the cross-sectional area are gradually increased along the spiral. In case of Radial type, the meridional velocity does not increase following with the increasing cross-sectional area, but is uniform. Then, the vertical velocity in the cross-sectional area is varied along the curved part of the rearguider and this may cause the friction loss.

Aforementioned, the eccentric vortex is an important parameter on the design of CFF and the recirculation induced by the eccentric vortex makes it difficult to determine the design flow rate in the design process. It is also noted that the distance from the eccentric vortex to the stabilizer is important for improving the performance. If the position of this vortex is located near the stabilizer, the performance becomes higher as generally known. As the setting angle is smaller, the distance becomes smaller because the eccentric vortex hardly moves. This reduces the recirculation quantity. Therefore, in case of the smallest setting angle, the performance is better than the others.

The fluid diffused from the main flow is discharged to the top of the impeller and some of that flows out to the inlet of the CFF. This may result in the increment of the loss and the unsteadiness. In case of 2nd Ar that has the small starting angle of the rearguider as shown in Fig. 1(b), the quantity of the diffusion flow is smaller than the others and suction and diffusion flows increase simultaneously. Therefore, the starting angle of the rearguider should be considered to reduce the diffusion flow.

5.2 Experimental results

In order to investigate the shape effects of the curved parts of rearguider, the pressure coefficient with the flow coefficient is plotted in Fig. 6. It is seen that the maximum pressure coefficient occurred at the design point (ϕ=0.51) and the pressure coefficient increases after decreasing on the left side of the design point. This is a general phenomenon for the multi-blade fan like the sirocco fan and may result from the strong unstable flow fields that induce a stall

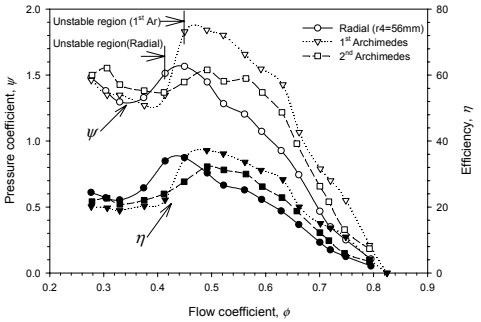

Fig. 6. Pressure coefficient and efficiency with flow coefficient for various rearguider types at 21° stabilizer position.

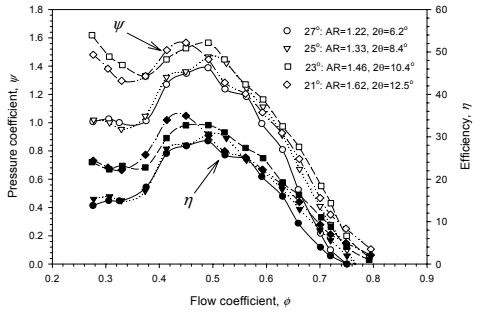

(a) Radial type rearguider

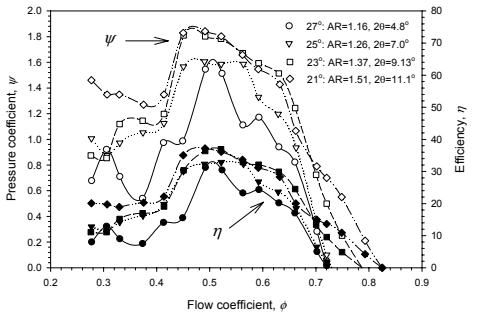

(b) 1st Archimedes type rearguider

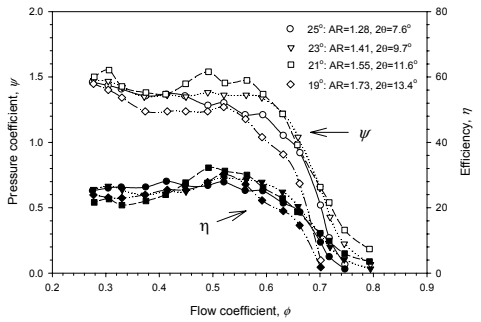

(c) 2nd Archimedes type rearguider

Fig. 7. Pressure coefficient and efficiency with flow coefficient for various stabilizer positions.

at the low flow rate. The stall causes loss and makes the difference of the pressure coefficient smaller.

The unstable region (±0.15 mmH_2O for radial type and ±0.20 mmH_2O for 1st Ar) occurred at the smaller flow coefficient than ϕ=0.45 (Radial type) and 0.49 (1st Ar), respectively. However, this region is barely generated for 2nd Ar. The instability reduction for 2nd Ar results from the decrement of the diffusion flow because of the small θ_{rs}. The flow is stable at the high flow rate and the pressure coefficient is higher in order: 1st Ar, 2nd Ar and Radial type. The 1st Ar makes the pressure coefficient 12% and the efficiency 8% higher than those of Radial type.

The operating characteristics with various positions of the stabilizer are shown in Fig. 7. The working fluid passes the first blade cascade through the right side of the impeller and enters the second cascade of the left side. The fluid obtains the momentum from the centrifugal force and the Coriolis force generated by the rotation of the impeller. The working fluid is also discharged into the rearguider within the discharge region (θ_d). However, some of the discharged fluid is recirculated to the impeller, which will result in the eccentric vortex. This vortex occurs necessarily when a cross-flow fan operates. The recirculation is an essential factor to produce the loss of a cross-flow fan. As the setting angle decreases, the inlet area of the diffuser (t_4) is decreased and much less flow is recirculated. The best setting angles (θ_{es}) having the highest ψ are 23° for Radial type, 21° for 1st Ar and 21° for 2nd Ar. The notion about the optimum setting angle is very obscure since there is no relevant design theory. As mentioned above, it is reasonable to define the region between the rearguider straight part and the stabilizer as a simple channel diffuser and find out the optimum area ratio (AR) and the enlargement angle ($2\theta_e$) of the diffuser. Because of the step-shear velocity distribution at the inlet of the diffuser, the best AR is respectively shown as 1.46, 1.51, and 1.55 in order: Radial type, 1st Ar and 2nd Ar. It is also noted that the best $2\theta_e$ is separately 7.4°, 11.1°, and 11.6°.

6. Conclusions

Flow behaviors in CFF with various shapes of the rearguider and setting angles of the stabilizer are studied. Following conclusions are obtained:

(1) The rearguider with Archimedes spiral shows a good way to raise the pressure coefficient and efficiency, comparing with the radial type.

(2) The starting angle of the rearguider is the important parameter to determine the diffusion flow and the stability at low flow rate.
(3) As the setting angle decreases, the inlet area of the diffuser is decreased. In that case, much less flow is recirculated to the impeller. This phenomenon may reduce the loss and lead to increase the velocity in the whole domain.

Nomenclature

b : Width [*mm*]
C : Absolute flow velocity [*m/s*]
M : Mach number
U : Absolute impeller velocity [*m/s*]
W : Relative flow velocity [*m/s*]
Z_b : Number of blade [-]

Greek symbols

α : Flow angle [*degree*]
β : Blade angle [*degree*]
θ_{es} : Setting angle of a stabilizer [*degree*]
θ_{rs} : Starting angle of a rearguider [*degree*]
σ : Slip factor [-]

Subscripts

2 : Exit of impeller
3 : Basic circle of a rearguider
d : Design point
m : Direction of radius
θ : Tangential direction

References

[1] B. Eck, Fans: Design and Operation of Centrifugal, Axis-Fan and Cross-Flow Fan, Pergamon press, New York, USA, (1973).
[2] H. Tsurusaki, Y. Tsujimoto, Y. Yoshida and K. Kitagawa, Visualization measurement and numerical analysis of internal flow in cross-flow fan, *Journal of Fluids Engineering* 119 (1997) 633-638.
[3] S. Yamafuji and K. Nishihara, 1976, An experimental study of cross flow fan, *Bulletin of JSME* 19 (129) (1976) 314-32.
[4] S. Murada and K. Nishihara, An experimental study of cross flow fan (1st report, effects of housing geometry on the fan perforamnce), *Bulletin of JSME* 19 (129) (1976) 314-321.